RSC Advances

PAPER

View Article Online
View Journal | View Issue

Cite this: *RSC Adv.*, 2026, **16**, 1038

Effect of palladium-doped magnetite nanoparticles in the hydrothermal liquefaction of biomass to bio-oil

Adson Tumwebaze,[ab] Edward Mubiru[a] and Dan Egesa*[a]

In this work, the mixed spent grain biomass, a mixture of maize and barley, was used as a feedstock for bio-oil production through hydrothermal liquefaction (HTL) in the presence of palladium-doped magnetite nanoparticle catalysts. The palladium-doped magnetite nanoparticles were synthesized by the co-precipitation process and characterized using Fourier transform infrared spectroscopy, transmission electron microscopy, and X-ray diffraction techniques. A maximum bio-oil yield of 61.3% was obtained using palladium-doped magnetite particles compared to 46.31% obtained in the absence of the catalyst. The elemental analysis of bio-oil showed an increase in elemental carbon from 55.07 wt% for uncatalyzed liquefaction to 76.47 wt% for Pd-doped magnetite nanoparticle-catalysed liquefaction. Similarly, the elemental hydrogen increased from 5.32 wt% for uncatalyzed to 7.63 wt% for Pd-doped magnetic nanoparticle catalysed liquefaction. The elemental analysis further indicated improved bio-oil quality, with a reduction in oxygen content from 36.52 wt% to 14.33 wt% and nitrogen from 2.51 wt% to 1.32 wt%. The GC-MS showed an increase of hydrocarbons from 60.45% for uncatalyzed liquefaction to 88.03% for Pd-doped magnetite nanoparticle catalysed liquefaction. Furthermore, the bio-oil produced in the presence of Pd-doped magnetite nanoparticles showed that physical properties were within acceptable limits compared to the crude bio-oil standard. The application of palladium-doped magnetite nanoparticles in the HTL of mixed spent grain biomass increases the yield of bio-oil and improves its quality, thus increasing its energy performance. This provides a potential pathway to produce a high-quality bio-oil suitable for blending or direct use in existing fuel systems.

Received 5th July 2025
Accepted 15th December 2025

DOI: 10.1039/d5ra04810a

rsc.li/rsc-advances

Introduction

The non-renewability of fossil fuels, the growing energy demand, and the increasing concerns about sustainability have promoted a huge interest in finding alternative energy sources.[1] This has led to the use of biomass as a feedstock for biofuel production, replacing fossil-based fuels.[2] Biofuel is a gaseous, liquid, or solid fuel produced from biomass. The biofuels are grouped according to the source of biomass.[1,3] The first generation is produced from edible biomass like maize and beans.[1,4] The second-generation biofuels are produced from largely inedible lignocellulosic materials, including jatropha and candlenut seeds, and municipal solid waste.[1,3] The third-generation biofuels are produced mainly from algal biomass.[1,5] The first-generation biomass is mainly utilized to feed human beings and is very limited in meeting the demand of the growing human population. The limited supply of food feedstock limits its utilisation to produce energy.[1] The second and third-generation biomass is considered the best alternative because of its wide availability, no competition for food, and being cheap.[1,5]

The mixed spent grain biomass is an example of lignocellulosic residue, used in this study. It is a mixture of maize and malt residue waste. The mixed spent grain biomass is one of the most abundant by-products generated from the beer brewing process, representing approximately 85% of the total by-products produced.[6] Therefore, using spent grain to produce the needed green energy is a better alternative for the environment.[7] The bio-oil produced is a valuable product in the economy that provides more income than the use of biomass as a feedstock.

Noting, it's high in cellulose, hemicellulose, and lignin, which makes it a potential feedstock for thermochemical technologies.[8] Gasification, direct combustion, pyrolysis, and hydrothermal liquefaction (HTL) are the most developed thermochemical technologies, which produce syngas (H_2 and CO), heat, and bio-oil, respectively, through the conversion of various biomass.[9] However, gasification, combustion, and pyrolysis are energy-intensive processes due to the pre-drying of feedstocks with high water content.[10] Thus, hydrothermal liquefaction is a preferred technology that converts higher water-content biomass feedstocks to bio-oil without the need for drying, potentially making the process efficient. Hydrothermal liquefaction is a high-temperature (200–400 °C), high-pressure (4–30 MPa) conversion process that produces liquid bio-oils directly

[a]*Department of Chemistry, College of Natural Sciences, Makerere University, P. O. Box 7062, Kampala, Uganda. E-mail: dan.egesa@mak.ac.ug*
[b]*National Environment Management Authority, P. O. Box 22255, Kampala, Uganda*

from solid biomass in the presence of water.[11,12] Water as a solvent has several advantages close to its critical point, leading to better solubility of organic compounds and high catalytic activity.[11,13] The HTL process gives a solid residue (char), a gaseous phase, and an organic liquid phase (bio-oil).[11] The obtained bio-oil is a potential alternative to conventional fossil fuels, but there are currently challenges to obtaining good-quality bio-oil from biomass.[14] The major challenges of bio-oil production from HTL are low conversion efficiency and the presence of high amounts of heteroatoms (N and oxygenated compounds), which lower the bio-oil yield and quality, respectively.[15] Researchers in recent years have done several studies on the HTL process, and a promising route has been the use of different catalysts to improve the yield and quality of HTL products.[4,16,17] Catalysts are either homogeneous or heterogeneous.[17] Homogeneous catalysts have been mostly used in the HTL process, including alkali, acids, and metal salts, to produce bio-oil.[18] However, their possible corrosiveness to the reactor and difficulty in recovery from the aqueous phase have reduced their application, directing attention to heterogeneous catalysts.[17,19]

Accordingly, the heterogeneous catalysts are easily recyclable and reused, and have been highly investigated recently for use in the HTL process.[2,19,20] Several categories, including the noble, redox, and transition metals, have been used in the catalytic conversion of biomass.[21] The HTL of macroalgae over a Fe_2O_3 was conducted by Rojas-Pérez *et al.*,[22] leading to a higher bio-oil yield, low corrosion, higher heating value, and reusability. Bi *et al.*[4] conducted a study of hydrothermal liquefaction on sweet sorghum bagasse in subcritical water in the presence of Ni/Si–Al catalyst and obtained bio-oil with improved viscosity, acid value, and water content, and an improved bio-oil yield of 45.0 wt%. In addition to increasing the bio-oil yield, supported heterogeneous catalysts using metal nanoparticles have exhibited a higher contribution to catalytic activity, reusability, and stability in the thermochemical reactions.[2,3,19,23] Egesa *et al.*[3] applied magnetite nanoparticles in the hydrothermal liquefaction of water hyacinth and obtained biocrude oil of higher yield (58.3 wt%) with higher carbon content and reduction of hetero atoms. The zero-valent metals, such as Zn, Al, and Fe, which are stable in water at ambient temperature but can react with water under hydrothermal conditions, have been investigated for the hydrothermal liquefaction process.[19] However, these traditional heterogeneous catalysts often cause over-hydrogenation, resulting in low selectivity.[24] In this regard, developing catalysts that can selectively produce high-quality bio-oil with low hetero atom content remains a major challenge for the HTL process.[25] There is a need to use suitable catalysts that improve biomass depolymerization and promote selective hydrogenation, deoxygenation, and desulfation to reduce the cost of subsequent upgrading processes.[26]

In some reported studies, palladium-based catalysts have been widely used in metal–organic chemistry,[27] and they present great performance in reactions such as hydrogenation, oxidative dehydrogenation, coupling, and desulfation.[24] Due to their unique electronic structures and their ability to adsorb and activate hydrogen and unsaturated substrates,[28] palladium-based catalysts are widely used in hydrogenation reactions.[24] Palladium (Pd) is chosen for its high cracking and hydrogenating activities, in addition to catalytic activity and stability.[29] Therefore, Pd is a potential catalyst immobilized on the surface of magnetite nanoparticles. Magnetite nanoparticles (Pd/Fe_3O_4) have gained attention due to their ability to accelerate catalytic activity, their high surface area, and easy recovery using a magnetic field,[30] which reduces mass transfer restrictions, allowing high concentrations of active sites per material mass.[31] No study has yet demonstrated the application of palladium-doped magnetite nanoparticles in the hydrothermal liquefaction of mixed spent grain. Therefore, the application of a tandem catalytic system provides a potential pathway, allowing for the advantage of the synergy between different active sites and reaction mechanisms to reduce the formation of heteroatoms. This study proposes the joint use of Pd/Fe_3O_4 catalysts and evaluates their catalytic effect in the hydrothermal liquefaction of mixed spent grain to bio-oil. This work extends the current literature and knowledge contributing to the development of a more efficient HTL process to produce a high-quality bio-oil.

Materials and methods

Synthesis of magnetite nanoparticles

The magnetite nanoparticles were prepared by following a previously reported literature procedure.[18] 8 g of hydrated iron(II) sulphate and 2.8 g of hydrated iron(III) sulphate were dissolved in 25 cm^3 of 0.2 M HCl in a beaker. 200 cm^3 of 1.5 M ammonium hydroxide solution was added dropwise to the resultant solution with vigorous stirring for 2 hours. The black precipitate was decanted from the solvent magnetically, and the catalyst was washed with ethanol. The catalyst was dried at 70 °C for 4 hours.

Synthesis of palladium-doped magnetite nanoparticles

The palladium-doped magnetite nanoparticles were prepared by following the previously reported literature procedure with slight modifications.[32] 0.5 g of magnetite nanoparticles was dispensed in 75 ml of distilled water and sonicated for 30 minutes in a separate beaker. In another beaker, 0.164 g of palladium chloride was dissolved in an acidic solution containing 100 μL of HCl in 10 ml of water. The contents of both beakers were mixed into one beaker. Then, 25 ml of ethanol was added to the mixture with vigorous stirring at 300 rpm for 1 hour. Then, the solution containing 50 ml of 0.04 M sodium borohydride solution was added dropwise to the solution containing palladium ions and magnetite nanoparticles, and the mixture was stirred at 200 rpm overnight to complete the reaction. The palladium-doped magnetite nanoparticles were magnetically extracted from the solution, washed with water and ethanol to neutralize residual ions, and vacuum-dried.

Hydrothermal liquefaction of mixed spent grains

Hydrothermal liquefaction experiments were conducted in a 250 ml ZZKD stainless steel high-pressure batch reactor CJF-01 with an upper limit pressure and temperature of 5000 psi and 400 °C, respectively. The reactor was equipped with

a mechanical stirrer connected to an electric motor, a thermocouple connected to a control box, a pressure gauge, and gas inlet and outlet lines supported with a Swagelok ball valve. The depth of the reactor was 9 cm, and the stirrer impeller had a diameter of 3.2 cm. The reactor contained 20 g of dry biomass, a specified amount of catalyst, and was mixed with 100 g of distilled water. The reactor was stirred at 200 rpm and was heated to the specified reaction temperature for about 20 min. Once the rector reached the specified reaction temperature, it was held during a specified time within ±1 °C of the specified operating temperature as per experimental design. After the holding time, the reactor was cooled to room temperature by running cold water. The reactor gas was vented off, and the contents of the reactor were first filtered on a Whatman filter paper to separate the aqueous phase from the solid residue (char). The solid residues were extracted with dichloromethane (DCM) as a solvent to separate the bio-oil from the char. Then, the mixture was filtered on a Whatman filter paper to separate the bio-oil and DCM mixture from the char (Fig. 1). The char was dried at room temperature under air circulation until a stable weight was obtained. This was repeated with the aqueous phase. The DCM was separated from the bio-oil using a rotary evaporator BUCHI R-300 operated under vacuum conditions at 40 °C at a rotation of 30 rpm.

The weight of bio-oil was measured by subtracting the weight of the glass vial with bio-oil from the weight of the empty glass. The weight of the char was determined by subtracting the weight of dried filter paper with solids from the weight of empty dried filter paper. All experiments were performed in triplicate.

Recycling of catalyst nanoparticles

The palladium-doped nanoparticles were recovered using a method from ref. 3. The dry catalyst nanoparticles were suspended in deionized water and sonicated for 30 minutes. The biomass floated to the surface and was skimmed off, while the catalysts were collected magnetically. This process was repeated three times to ensure a biomass-free catalyst. The recovered nanoparticles were then weighed and reused in additional HTL reactions under similar conditions.

Analytical techniques

Surface morphology and size of the nanoparticles were analysed using a JEM1200 EX11 transmission electron microscope (TEM) at a 300 kV voltage. The nanoparticle catalyst powder was dispersed in 99% ethanol to form a suspension. Image J software was used to determine the size distribution of the magnetic nanoparticles. The Bruker D8 advanced X-ray diffractometer (XRD), operated at 40 kV and 80 mA and a scanning rate of 0.02°

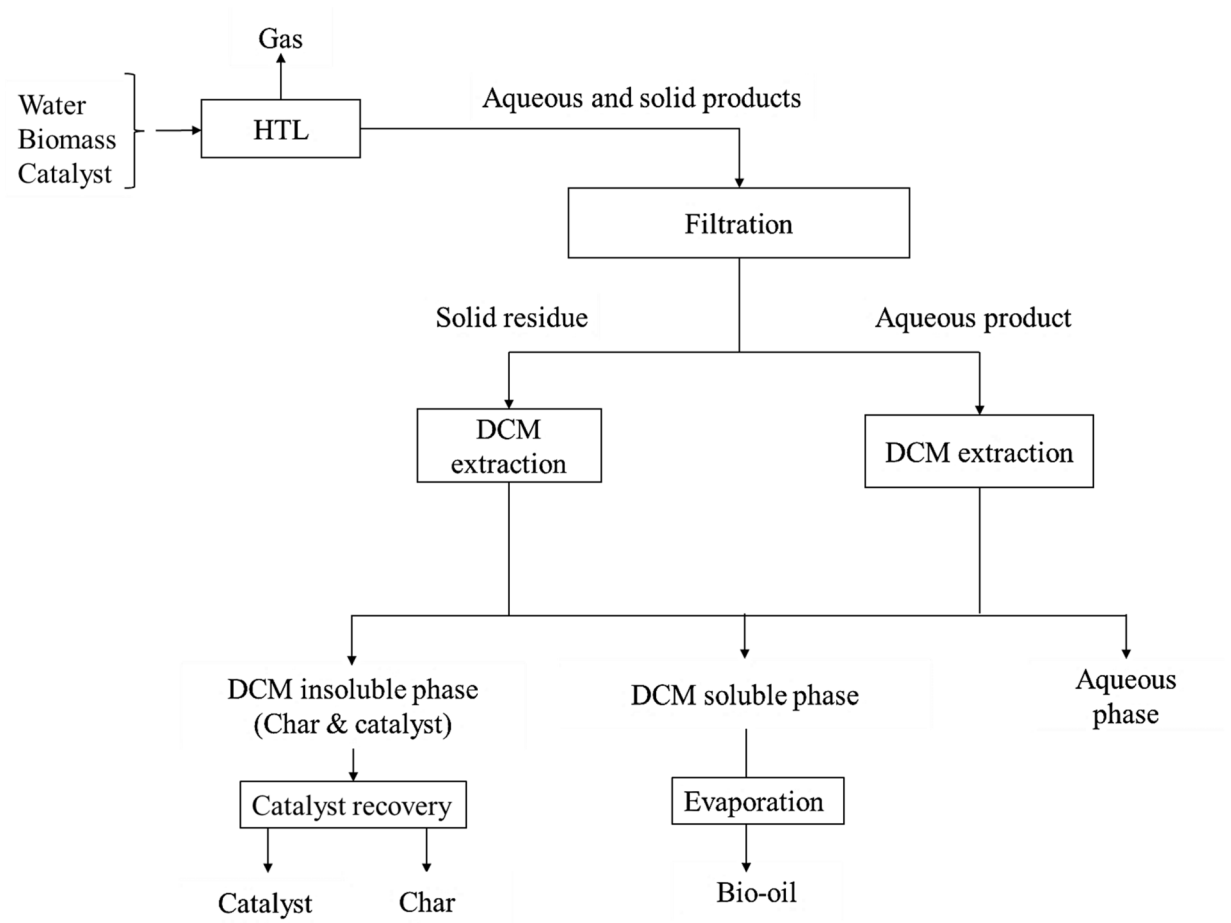

Fig. 1 Experimental flow chart of the HTL process and separation of products.

s^{-1} in 2θ from 20° to 70°, was used to analyze the crystallinity of the nanoparticles. The elemental composition of the nanoparticles was analysed using an energy-dispersive X-ray fluorescence spectrometer (EDX-8100, Shimadzu, Japan). The spectrometer was equipped with five primary filters and a high-resolution camera for sample positioning, fitted with a high-performance silicon drift detector along with a PCEDX Pro software for analysis, optimization, and data analysis. Before analysis, the equipment was calibrated using the standard A750. The bio-oil was analysed for elemental composition (H, N, S, O, C) in triplicate using a Thermo Fisher Flash 2000 elemental analyser using the Xperience software that provided peak values in the form of percentages for carbon, nitrogen, sulphur, and hydrogen. The oxygen content percent was obtained by difference. GC-MS analysis to determine compounds in the bio-oil was performed on a Shimadzu gas chromatograph coupled to a mass-spectrometer selective detector. Chromatographic separations were achieved on a fused-silica capillary column (DB5) of length 30 m, 0.25 mm internal diameter, and thickness of 0.25 μm. The chromatographic conditions for GC-MS analysis were the injector temperature at 200 °C; the transfer line temperature was 250 °C, the initial oven temperature was 50 °C hold for 1 minute, and the heating rate was 20 °C $minute^{-1}$ up to 140 °C and no holding and then 10 °C $minute^{-1}$ up to the final temperature of 300 °C and hold for 10 minutes. The carrier gas was helium (99.999% purity) at a flow rate of 1.69 ml $minute^{-1}$. The analysis of bio-oil composition was performed in the scan mode at a mass range of 50–480 *m*/*z*. The identification of bio-oil compounds was obtained by comparing mass spectra included in the NIST20 library.

Bio-oil analysis

The percentage yield of bio-oil was calculated according to eqn (1), on an ash and moisture-free basis, based on previous studies.[3,18,33–35]

$$Y_P = \frac{W_P}{W_{SG} - W_A - W_M} \times 100\% \quad (1)$$

where Y_P is the percentage yield of the product, W_P is the weight of the product (g), W_{SG} is the weight of the mixed spent grain fed into the reactor, and W_A and W_M are the ash and moisture content of the mixed spent grain, respectively.

The higher heating values of the bio-oil were calculated using the Dulong formula as shown in eqn (2).

$$HHV(MJ\ kg^{-1}) = 0.3383C + 1.428\left(H - \frac{O}{8}\right) + 0.095S \quad (2)$$

where: HHV is the high heating value, C, H, and O are the wt% of carbon, hydrogen, and oxygen present in the product.

The flash point of the bio-oil was measured using the NPM 450 flash point analyser in compliance with the standard test method ASTM D93 (ref. 36). The kinematic viscosity of the bio-oil was measured by following the standard test method ASTM 445 using a Ubbelohde glass (PSL Rheotek) viscometer. The total acid number of the bio-oil was measured according to the generic European standard EN14104, 2003. The iodine value was determined according to ISO 3961 (ref. 37) and previously utilised by Adeyemi *et al.*[38]

Results and discussion

Synthesis and characterisation of nanoparticles

TEM images (Fig. 2A) showed that the magnetite nanoparticles were crystalline and monodisperse, with particle sizes ranging between 6 and 14 nm, and an average particle size of 10.5 nm, as measured using ImageJ software. The palladium-doped nanoparticles had better crystallinity, higher intensity, and an increased particle size between 10 and 18 nm (Fig. 2B) with an average particle size of 14.2 nm as analysed using Image software (Fig. 3). The powder XRD results confirmed the increase in particle size due to doping, which showed increased intensity and sharpening of peaks. The sharpening of peaks is a clear indication of doping with Pd. The major diffraction peaks, which correspond to Pd-doped magnetite, were at $2\theta = 35.83°$, 43.502°, and 63.069°, corresponding to the (111), (200), and (220) crystal planes of Pd-doped nanoparticles (Fig. 5), which are closely consistent with JCPDS (no. 05-0681). The results agreed with similar studies reported in the literature on Pd nanoparticles with (111) at the highest.[39,40] The elemental composition of the synthesized Pd-doped magnetite nanoparticles was also confirmed using EDS (Fig. 4). The EDS analysis confirmed the presence of Pd in the doped samples. The results obtained from energy dispersive X-ray fluorescence spectrometry showed elemental composition of the nanoparticles with palladium (65.06%) as a major element, followed by iron (33.61%). Other impurities included silicon (0.20%), calcium (0.33%), sodium (0.45%), chromium (0.21%), and europium (0.14%). The FT-IR spectra had wide bands between 2650 and 3400 cm^{-1} indicated the –OH groups due to adsorbed water. The vibration bands appearing at 526 and 460 cm^{-1} are attributed to Pd-doped magnetite and magnetite nanoparticles, respectively (Fig. 6).

Catalytic effect of Pd-doped magnetite nanoparticles on the yield of bio-oil

The effect of catalyst dosage on the HTL of the mixed spent grain biomass was investigated when magnetite nanoparticles and palladium-doped magnetite nanoparticles were used. Fig. 7 shows the bio-oil yield from HTL of mixed spent grain biomass at various catalyst dosages of 0.0175 g g^{-1}, 0.0463 g g^{-1}, and 0.075 g g^{-1} at a constant holding time of 45 minutes and temperature of 290 °C, following the experimental design model by response surface methodology. The bio-oil yield increased from 43.5% to 48.2% and to 51.6% when the magnetite nanoparticles catalyst dosage was increased from 0.0175 g g^{-1} to 0.0463 g g^{-1} to 0.075 g g^{-1}, respectively. Similarly, when palladium-doped magnetite nanoparticle catalyst dosage was increased from 0.0175 g g^{-1} to 0.0463 g g^{-1} and then to 0.075 g g^{-1}, the bio-oil yield increased from 45.3% to 48.6% to 48.9%, respectively.

Similar trends have been observed in some studies involving the application of catalysts in the HTL of related feedstocks. A study by Zhao *et al.*[20] showed that the bio-oil yield increased from 24.81% to 36.82% as iron catalyst dosage was increased from 0% to 10%. The influence of iron was attributed to the reactive intermediates formed from biomass depolymerization stabilized by *in*

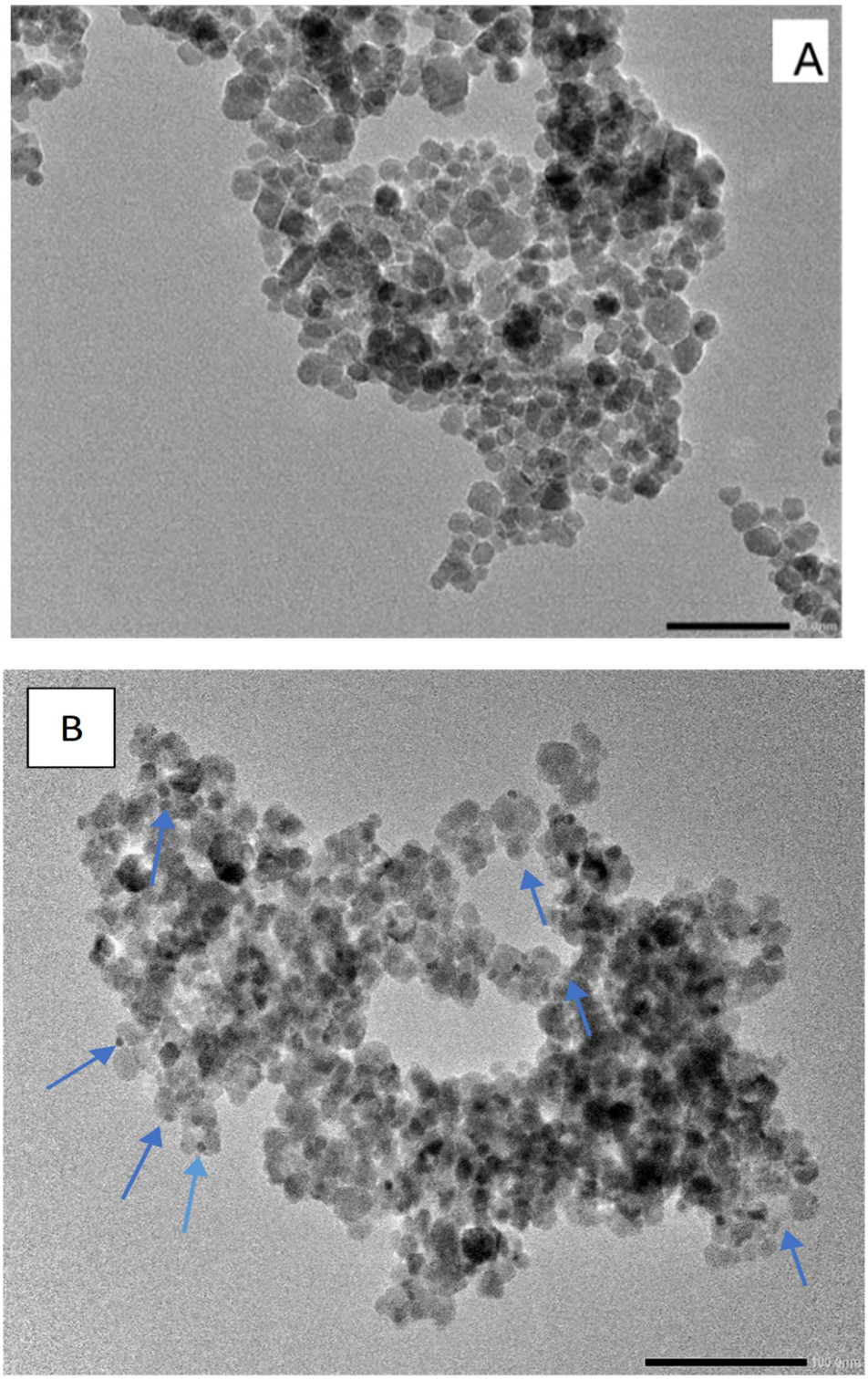

Fig. 2 TEM images for nanoparticles: (A) – undoped magnetite, (B) – Pd-doped magnetite (with arrows indicating Pd on magnetite).

situ hydrogen reaction with iron. de Caprariis *et al.*[41] observed that loading of iron catalyst improved bio-oil yield by 20% during the HTL of oak wood when the iron amount was increased from 0.05 mg to 0.1 mg. This is similar to our study. This was also attributed to the reactions of iron with intermediates to produce hydrogen, which inhibits the condensation and repolymerization of bio-oil compounds, thus enabling a high bio-oil yield. The increase of bio-oil from 43% to 58.8% was observed when the magnetite nanoparticles were increased from 0 g g^{-1} to 0.2 g g^{-1} during the liquefaction of water hyacinth.[3] This was due to the

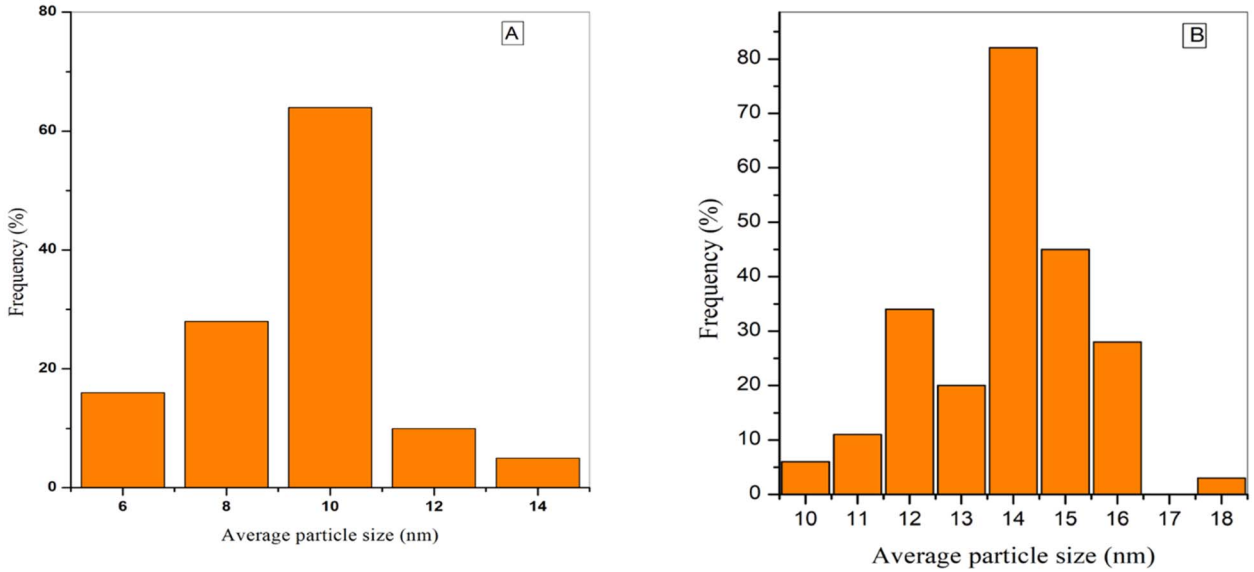

Fig. 3 Particle size distribution of nanoparticles; (A) – magnetite, (B) – Pd-doped magnetite.

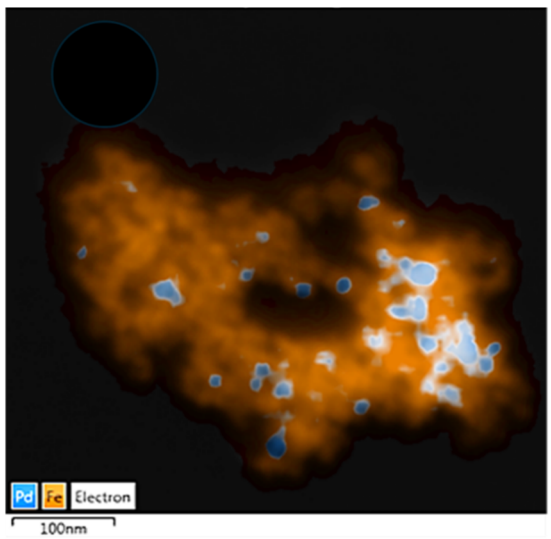

Fig. 4 EDS mapping showing the elemental distribution of Pd over magnetite nanoparticles.

maximum exposure of catalyst active sites for biomass conversion, leading to increased yield and reduced char,[3] which is comparable with this study. There was an insignificant 0.62% increase in bio-oil yield when the palladium-doped magnetite nanoparticles catalyst dosage was increased from 0.0463 g g^{-1} to 0.075 g g^{-1}. This is attributed to increased particle aggregation at higher concentrations.[3] Under these experimental conditions, the catalyst dosage of nanoparticles was 0.075 g g^{-1} to obtain maximum bio-oil yield.

Catalyst recovery and re-use for HTL

After magnetic separation of nanoparticles from the char phase, the clean nanoparticles were subjected to HTL. The recovered nanoparticles were then weighed and reused in additional HTL reactions under similar conditions of 0.075 g g^{-1} at 320 °C for 60 minutes. After completing the first set of experiments, the same catalyst was recovered and reused for HTL under the same conditions. In the first cycle, the nanoparticles showed a yield of 45.1%, which was 3.8% less than the fresh catalyst. The catalysts were used up to three recycles (Fig. 8). The results showed that the reuse of palladium-doped magnetite nanoparticles was efficient; however, their reusability in terms of bio-oil yield decreased as the number of cycles increased. This is attributed to structural changes through particle size variation and increasing mass volume ratio.[18] Therefore, recycling of the nanoparticles could result in lowering the processing cost of bio-oil and potentially making biofuels more competitive.

Effect of Pd-doped magnetite nanoparticles on the chemical composition of the bio-oil

The catalytic effect of Pd-doped magnetite nanoparticles on the chemical composition of bio-oil was determined by elemental analysis and GC-MS.

Elemental analysis of bio-oil

The elemental analysis of bio-oil from mixed spent grains liquefaction was compared at 320 °C without a catalyst dosage of 0.075 g g^{-1} of magnetite nanoparticles and palladium-doped magnetite nanoparticles (Table 1) at 60 minutes. This was based on the fact that under these conditions, the highest bio-oil yield was achieved.

Overall, the amount of hydrogen and carbon in the bio-oil was much higher than in the biomass feedstock. The carbon content of bio-oil increased from 43.17 wt% in the spent grain feedstock to 55.07 wt% in un-catalysed bio-oil and 64.13 wt% in magnetite nanoparticles catalysed bio-oil. The hydrogen content increased from 4.07 wt% in the spent grain feedstock to 5.32 wt% in un-catalysed HTL. The bio-oil produced in the presence of catalysts contained higher compositions of carbon and hydrogen than bio-

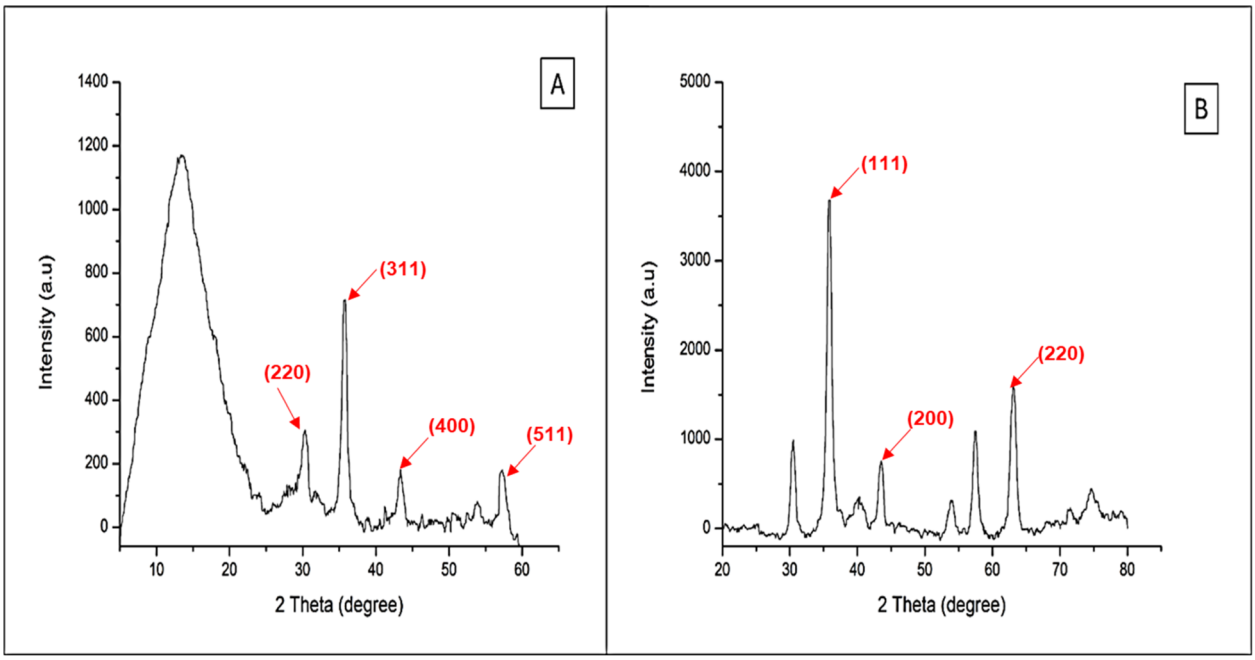

Fig. 5 XRD patterns of the nanoparticles: (A) – magnetite; (B) – Pd-doped magnetite.

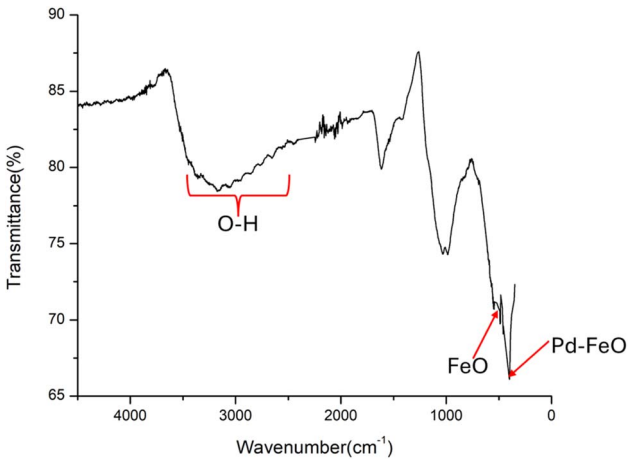

Fig. 6 The FT-IR spectrum for Pd-doped magnetite nanoparticles.

oil produced in the absence of the catalyst. This is in agreement with the findings of ref. 18 on the effect of magnetite nanoparticles on microalgae biomass liquefaction. The bio-oil produced in the presence of the palladium-doped magnetite nanoparticles had a higher carbon content of 76.47 wt% than the 64.13 wt% in the magnetite nanoparticles catalysed HTL. A similar trend was observed with the hydrogen content in bio-oil catalysed by palladium-doped magnetite nanoparticles of 7.63 wt%, higher than 6.17 wt% of magnetite nanoparticles catalysed HTL. The synergetic effect in palladium-doped magnetite modifies the electronic sites of iron, thus enhancing redox reactions and improving catalytic selectivity toward hydrocarbons. In addition, palladium has a higher hydrogen dissociation ability during the water–gas shift reactions in HTL, more efficiently than iron alone. Palladium catalyses hydrodeoxygenation reactions by exploiting the H_2 produced from Fe oxidation and cellulose decomposition, thus obtaining more stable water-soluble compounds in the bio-oil. Therefore, this indicates that the HTL of mixed spent grain in the presence of palladium-doped magnetite nanoparticles leads to an increase in the hydrogen and carbon content of bio-oil.

The amount of nitrogen and oxygen in the biomass feedstock was much higher than in the bio-oil. The oxygen content was reduced from 45.76 wt% in the biomass feedstock to 36.52 wt% in bio-oil from uncatalyzed HTL to 27.19 wt% in bio-oil from magnetite nanoparticles catalysed HTL, and to 14.33 wt% in bio-oil from palladium-doped magnetite nanoparticles catalysed HTL. Deoxygenation occurs through the release of oxygen into the gas phase as carbon dioxide and carbon monoxide.[42] Consequently, the 60-minute holding time facilitated the transfer of oxygen to the gas phase, resulting in a higher rate of deoxygenation. The results indicated that the Pd-doped magnetite nanoparticles potentially played a catalytic role by favouring the deoxygenation reactions,[43] resulting in faster removal of oxygen from bio-oil.

The nitrogen content was reduced from 6.29 wt% in the biomass feedstock to 2.51 wt% in bio-oil from un-catalysed liquefaction to 2.08 wt% bio-oil from magnetite nanoparticles catalysed HTL, and to 1.32 wt% bio-oil from palladium-doped magnetite nanoparticles catalysed HTL. A similar reducing trend of nitrogen in the presence of catalysts was also observed in the studies on HTL for similar biomass.[3,44] The reduction of nitrogen content may be due to the partitioning of nitrogen in the aqueous phase as ammonia.[42] The results indicate that the Pd-doped magnetite nanoparticles favoured the loss of nitrogen into the aqueous phase at a reaction time of 60 minutes. Denitrogenation improves the HHV of bio-oil and reduces the release of harmful nitrogen oxide gases into the atmosphere.[42] The presence of a high content of hetero atoms (N and O) in the bio-oil leads to undesirable fuel

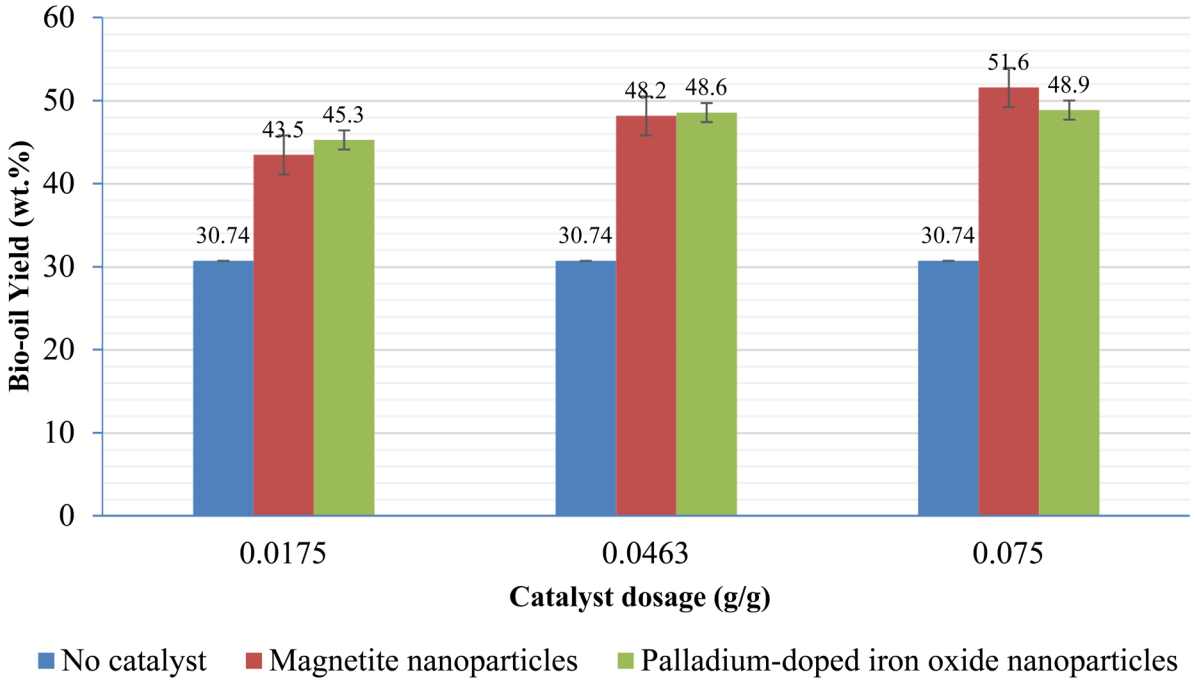

Fig. 7 Effect of catalyst dosage on bio-oil yield at constant temperature and holding time.

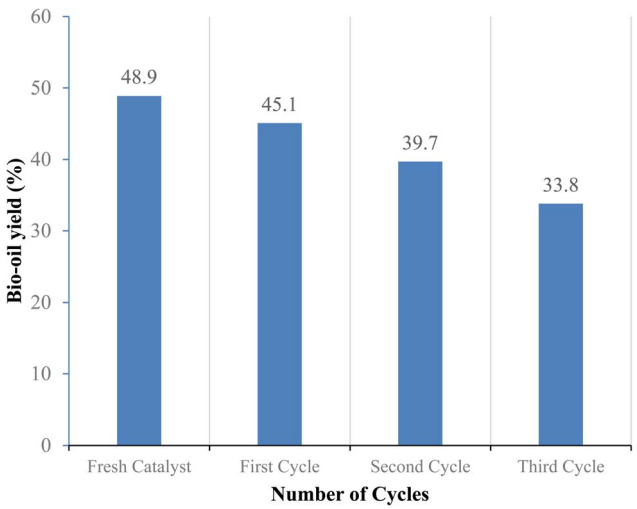

Fig. 8 A comparison of bio-oil yields for fresh and recycled catalysts in HTL.

properties, such as acidity and high viscosity, that result in negative effects on storage and combustion performance.[3,45] The further reduction in oxygen and nitrogen contents of bio-oil in the catalysed HTL shows that the presence of palladium-doped magnetite nanoparticles plays a major role in deoxygenation and denitrogenation of bio-oil[43] and thus can potentially be used as HTL catalysts to improve the quality of bio-oil.

The sulphur content reduced from 0.71 wt% in the biomass feedstock to 0.58 wt%, 0.43 wt%, and 0.25 wt% in bio-oil liquefied in the absence of a catalyst, presence of magnetite, and palladium-doped magnetite nanoparticles, respectively. This indicated that there was an increasing desulphurization with the addition of catalysts.[42] More sulphur was removed in the presence of Pd-doped magnetite nanoparticles. This confirms that the Pd-doped magnetite nanoparticles had a catalytic role in desulphurization reactions. A high sulphur content in bio-oil leads to the production of harmful gases, such as sulphur dioxide gas which leads to the formation of acid rain.

The HTL in the presence of the nanoparticles led to the highest high heating value (HHV) of 34.23 MJ kg^{-1} with

Table 1 The elemental composition, atomic ratios, and high heating values (HHV) of bio-oil

	Elemental composition					Atomic ratios of elements			
Bio-oil sample	C (wt%)	H (wt%)	N (wt%)	O[a] (wt%)	S (wt%)	N/C	H/C	O/C	HHV (MJ kg^{-1})
No catalyst	55.07	5.32	2.51	36.52	0.58	0.04	1.16	0.50	19.76
Magnetite nanoparticles	64.13	6.17	2.08	27.19	0.43	0.03	1.15	0.32	25.69
Palladium-doped magnetite nanoparticles	76.47	7.63	1.32	14.33	0.25	0.01	1.20	0.14	34.23

[a] Obtained by difference.

palladium-doped nanoparticles and 25.69 MJ kg^{-1} with magnetite nanoparticles in comparison with bio-oil from the un-catalysed liquefaction (19.76 MJ kg^{-1}). This also indicates the highest energy recovery for liquefaction in the presence of nanoparticles. Doping magnetite with palladium improved the HHV of the bio-oil compared to only the use of magnetite by a 25.18% increase. This is brought about by the low heteroatom content and higher oxygen and carbon in bio-oil. Palladium, like other metal support catalysts, promotes the selective hydrogenation reaction during liquefaction.[19] The incorporation of Pd onto magnetite leads to the isolation of Pd active sites that change the adsorption behaviour of intermediate products formed during liquefaction, which effectively inhibits reactions that lead to the formation of heteroatoms.[24] This shows that the Pd-doped magnetite nanoparticles have a larger influence on increasing the HHV of the bio-oils.

The H/C, N/C, and O/C atomic ratios for bio-oil were calculated as indicated in Table 1. The H/C ratio of feedstock (1.13) increased to 1.16 during the uncatalysed HTL and when magnetite was used. The ratio further increased to 1.20 when Pd-doped magnetite nanoparticles were used. The H/C ratio indicates the aromaticity of the bio-oil. Pd enhances selectivity for hydrocarbon formation, stabilizing intermediates such as ketones and aldehydes by converting them into alkanes and alcohols through hydrogenation. The higher the H/C ratio, the higher the energy performance of the bio-oil and the lower the carbon dioxide produced from its combustion, thus improving its quality.

The N/C ratio of feedstock (0.12) was reduced to 0.04 in uncatalyzed liquefaction, and further to 0.03 and 0.01 in magnetite and Pd-doped magnetite nanoparticles catalysed liquefaction, respectively. The N/C ratio indicates the amount of N and C in the bio-oil and is important to understand the solid content in the bio-oil. A high N is undesirable since it leads to the production of harmful nitrogen oxides during combustion. Pd enhances hydrodenitrogenation, where the carbon–nitrogen bonds are broken, and the nitrogen atoms are removed as ammonia in the presence of hydrogen. The results from this study indicate that the presence of Pd-doped magnetite nanoparticles leads to increased removal of N compounds from bio-oil, thus reducing the N/C ratio.

The O/C ratio of feedstock (1.06) was reduced to 0.5 in uncatalyzed liquefaction. It steadily reduced to 0.32 to 0.14 in magnetite and Pd-doped magnetite nanoparticles, catalysed liquefaction. The O/C ratio shows the polarity and abundance of polar oxygen-containing surface functional groups in bio-oil. A higher O/C ratio implies that there are more polar functional groups in the bio-oil, and a lower O/C ratio shows that there are fewer polar functional groups in the bio-oil. This indicates there is predominantly an adsorption mechanism based on van der Waals forces instead of ion exchange.[3] This confirms the lower viscosity of bio-oil since the sorption capacity within the bio-oil drops due to weaker van der Waals forces.

GC-MS analysis of bio-oil

The main individual groups were identified in the bio-oil from mixed spent grain, and their relative areas in the chromatogram after integration were determined. The analysis was done on bio-oils obtained at 360 °C for 60 minutes and with a catalyst dosage of 0.075 g g^{-1}. The peaks in the chromatogram with a relative area of less than 1% area were not considered. The major compounds in the bio-oil were grouped under hydrocarbons, nitrogen, and oxygenated compounds (Fig. 9). The hydrocarbon grouping consisted of aliphatic and aromatic hydrocarbons. The percentage of sulphur-containing compounds was too small to be detected.

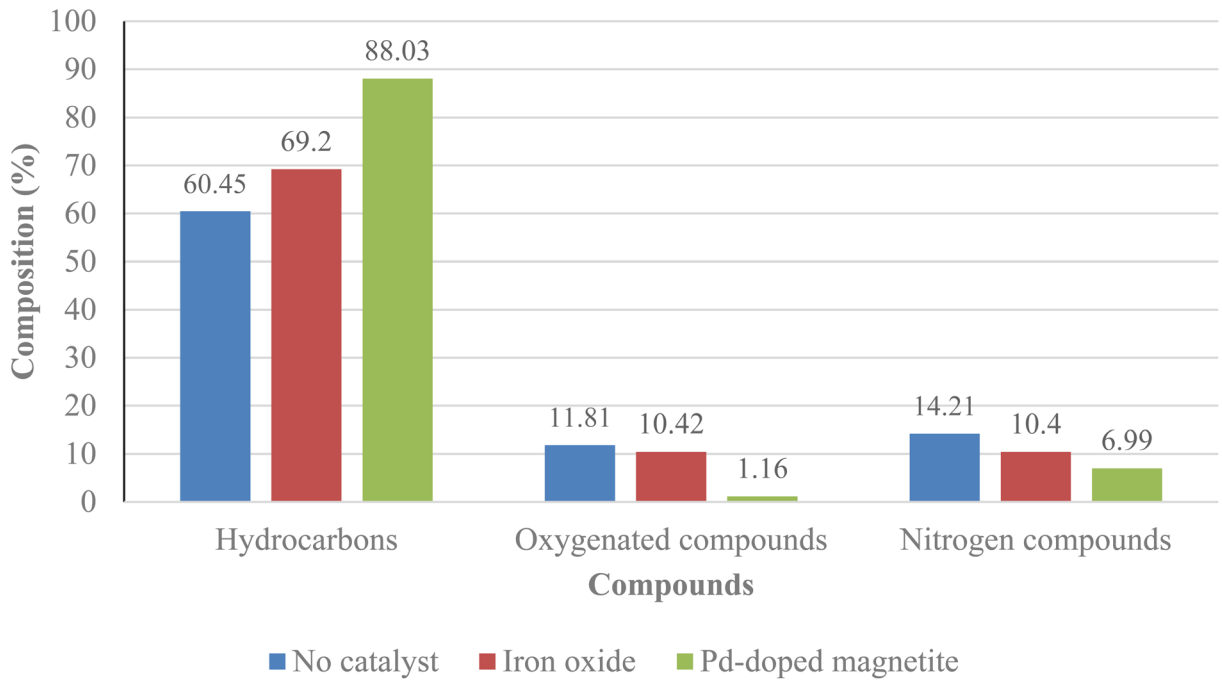

Fig. 9 Distribution of major compounds in bio-oil after HTL in the absence of a catalyst and presence of nanoparticle catalysts.

Table 2 The average values for the analysed parameters for bio-oil samples with biodiesel standards

Parameters	Bio-oil	Standard limit for biodiesel[47]
Kinematic viscosity at 40 °C ($mm^2\ s^{-1}$)	4.72 ± 0.11	1.9–6.0
Total acid number (TAN) (mg KOH per g)	0.32 ± 0.36	<0.5
Iodine value (g I_2 per 100 g oil)	122.64 ± 1.45	120–130
Flashpoint (°C)	146	130 (min)
Higher heating value (MJ kg^{-1})	34.23	37–40

The composition of compounds (Fig. 9) indicated that the bio-oil from un-catalysed liquefaction registered the lowest percentage of hydrocarbons (60.45 area%) while bio-oil produced in the presence of palladium-doped magnetite nanoparticles registered the highest percentage (88.03 area%). The increase in hydrocarbon composition in the presence of nanoparticles indicates a major catalytic role in promoting the decomposition of polymer components such as carbohydrates, lipids, and proteins.[3] The hydrocarbons from all bio-oils were mainly composed of alkanes, with heneicosane as the most predominant, as indicated in the SI. Others included pentadecane, hexadecane, heptadecane, nonadecane, eicosane, tetracontane, squalane, and tetracosane. A high percentage of heneicosane (26.66 area%) was observed with palladium-doped magnetite-catalysed liquefaction. The uncatalysed liquefaction had the lowest percentage of heneicosane (18.8 area%) in the bio-oil. These results indicate that the catalyst is aiding the deoxygenation of lipids into hydrocarbon species more effectively than the uncatalyzed liquefaction process.

The grouping of nitrogen compounds included: *N*-3-piperidiny propane, hexadecanamide, *N*-methyl arachidamide, *N*,*N*-dimethyl palmitamide, *N*-ethyl arachidamide, and *N*-3-methyl octanamide. The bio-oil from un-catalysed liquefaction contained more nitrogen compounds (14.21 area%) compared to magnetite nanoparticles (10.4 area%) and palladium-doped magnetite nanoparticles (6.99 area%). The higher nitrogen content is attributed to the protein content in the feedstock. The proteins undergo degradation through deamination, decarboxylation, depolymerisation, and dehydration to form nitrogen compounds.[17] The amount of nitrogen in the palladium-doped magnetite nanoparticles catalysed liquefaction was the lowest. This agrees with the elemental analysis results that show a general reduction in the percentage of elemental nitrogen in catalysed bio-oil. This confirms that Pd-doped magnetite nanoparticles play a catalytic role in removing nitrogen compounds from bio-oil to produce more water-soluble compounds, thus improving the bio-oil quality.

The grouping of oxygenated compounds included phenolic compounds, organic acids, and ketones. The phenol grouping only had 4-ethyl-2-methyl phenol and was observed in significant amounts in the bio-oil from the uncatalysed and magnetite nanoparticle liquefaction process. The amount of phenol in bio-oil catalysed by palladium-doped magnetite nanoparticles was below detectable levels. The grouping of organic acids included: methyl ester, hexadecenoic acid, *n*-hexadecanoic acid, octadecanoic acid, 1-ethynyl cyclododecanol, *cis*-vaccenic acid, nonahexacontanoic acid, and the ketone grouping, mainly contained dihydro-5-tetradecyl 2(3*H*)-furanone. The organic acids are due to the breakdown of glucose under hydrothermal liquefaction.[46] The oxygenated composition was lowest in bio-oil from HTL in the presence of palladium-doped magnetite nanoparticles. This is possible due to their catalytic effect in breaking down organic acids to hydrocarbons through the deoxygenation reaction pathway, as confirmed by the highest yield of hydrocarbons in the bio-oil (Fig. 9). This agrees with the elemental analysis results that revealed an oxygen reduction when mixed spent grain liquefaction was done in the presence of palladium-doped magnetite nanoparticles. The GS-MS and elemental analysis results demonstrate increased removal of heteroatoms from bio-oil using palladium-doped magnetite nanoparticles in HTL of mixed spent biomass.

Energy performance properties of the bio-oil

The energy performance properties for bio-oil obtained from HTL of mixed spent grain biomass in the presence of palladium-doped magnetite nanoparticles at 350 °C for 60 minutes and 1.5 g catalyst dosage were analysed. The results are shown in Table 2.

The kinetic viscosity of the bio-oil was 4.7 ± 0.11 $mm^2\ s^{-1}$, which falls within the acceptable limits of 3.5–5.0 $mm^2\ s^{-1}$ for crude biodiesel, as specified in ASTM 6751. The bio-oil indicates potential stability during storage. This means that the utilisation of bio-oil is economical and environmentally friendly, as it requires less energy to refine into fuel. Higher viscosity leads to poor atomization of the fuel, thus poor combustion and increased carbon monoxide.[45] The lower kinematic viscosity indicates the tendency of bio-oil to exhibit internal resistance to free motion.[48] The kinetic viscosity is an important specification for the fuel injectors used in fuel engines. The total acid number (TAN) of bio-oil was 0.32 ± 0.36 mg KOH per g, which was within permissible limits. This demonstrates that the bio-oil can be considered for upgrading. The acidity of bio-oil is due to the presence of long-chain fatty acids, phenolic, and carboxylate compounds.[48,49] High TAN leads to the corrosion of engine parts and storage facilities.[50,51] The results obtained mean that the bio-oil is free from corrosion properties at storage and while in the equipment system. The iodine value of bio-oil was 122.64 ± 1.45 g I per 100 g, which was within the permissible limits. The iodine value evaluates the bio-oil stability to oxidation.[48] The higher iodine value shows how easily it is oxidised in contact with air. The bio-oil with high iodine value tends to polymerize easily due to the high degree of unsaturation of the fatty acids. The iodine value result from this study indicates resistance to chemical changes during long-term storage and thus a high-quality bio-oil. The flash point was 146 °C, which was within the permissible limits. This is the minimum temperature at which the bio-oil will ignite on

application of an ignition source under specified conditions.[48] This means the bio-oil from palladium-doped magnetite catalysed HTL is safer to store and transport since the tendency of the sample to form a flammable mixture with air is minimal. Fuels with high flash points are less flammable, making the fuel safer to handle and store and less hazardous.[48]

Conclusion

In this study, palladium-doped magnetite nanoparticles were synthesised by co-precipitation and used to investigate their catalytic effect on the yield and chemical composition of bio-oil from hydrothermal liquefaction of mixed spent grain biomass. The palladium-doped magnetite nanoparticles exhibited an improved performance by producing the highest bio-oil yield of 61.3 wt%, which indicated an increase of 14.09 wt% when HTL was done in the absence of a catalyst. The elemental analysis of the bio-oil showed an increase in carbon content by 21.4% with Pd-doped magnetite nanoparticles. The GC-MS results indicated an increase in the percentage composition of hydrocarbons in the bio-oil by 27.58% in the presence of Pd-doped magnetite nanoparticles. Similarly, there was a reduction in the composition of oxygenated compounds by 10.65% and nitrogen compounds by 7.22%. This showed that the Pd-doped magnetite nanoparticles played a significant catalytic role in the hydrothermal liquefaction of mixed spent grain. Therefore, we have shown for the first time that the application of Pd-doped magnetite nanoparticles as a catalyst to use in the HTL process of mixed spent grain biomass increases yield and quality of bio-oil. Thus, developing a sustainable pathway for the conversion of MSG into bio-oil through HTL to minimise environmental impact by providing a cleaner, more efficient alternative to traditional fossil fuels.

Author contributions

Tumwebaze Adson: methodology, conceptualisation, validation, formal analysis, investigation, data curation, writing – original draft, writing – review & editing manuscript, visualization; Mubiru Edward: methodology, formal analysis, investigation, data curation, writing – review & editing and co-supervision; and Egesa Dan: conceptualization, methodology, formal analysis, resources, writing – review & editing, and supervision.

Conflicts of interest

The authors declare that there is no conflict of interest regarding the publication of this study.

Data availability

The authors confirm that all relevant data supporting the findings of this study are included within the submitted manuscript. If any additional raw data files in alternative formats are needed, they can be made available upon reasonable request from the corresponding author. The data from the GC-MS analysis supporting this article have been included as part of the supplementary information (SI). Supplementary information is available. See DOI: https://doi.org/10.1039/d5ra04810a.

Acknowledgements

The authors gratefully acknowledge the Uganda National Council for Science and Technology (UNCST) for providing funding for the reactor used and the department of Chemistry, College of Natural Sciences, Makerere University for providing laboratory and other instrumental facilities.

References

1 L. C. Energy, *et al.*, Progress in lignocellulosic biomass valorization for biofuels in the EU: a focus on thermochemical, *Sustainable Bioenergy Process*, 2024, **18**(3), 755–781, DOI: 10.1002/bbb.2544.
2 C. A. Moreira-mendoza, S. Essounani-m, S. Molina-ramírez, M. Cort and L. J. Alemany, Biocrude upgrading with tandem catalysts *via* hydrothermal liquefaction of biomass feedstocks, *Catal. Today*, 2025, **461**(8), 115496, DOI: 10.1016/j.cattod.2025.115496.
3 D. Egesa, P. Mulindwa, E. Mubiru, H. D. Kyomuhimbo and G. Aturagaba, Hydrothermal Liquefaction of Water Hyacinth: Effect of Process Conditions and Magnetite Nanoparticles on Biocrude Yield and Composition, *J. Sustainable Bioenergy Syst.*, 2021, **11**(04), 157–186, DOI: 10.4236/jsbs.2021.114012.
4 Z. Bi, *et al.*, Biocrude from pretreated sorghum bagasse through catalytic hydrothermal liquefaction, *Fuel*, 2017, **188**, 112–120, DOI: 10.1016/j.fuel.2016.10.039.
5 S. P. Singh and A. Golberg, *Hydrothermal Liquefaction: Biomass and Waste to Biofuels*, 2019.
6 S. Aliyu and M. Bala, Brewer's spent grain: a review of its potentials and applications, *Afr. J. Biotechnol.*, 2011, **10**(3), 324–331, DOI: 10.5897/AJBx10.006.
7 M. Carlini, E. M. Mosconi, S. Castellucci, M. Villarini and A. Colantoni, An economical evaluation of anaerobic digestion plants fed with organic agro-industrial waste, *Energies*, 2017, **10**(8), 1165, DOI: 10.3390/en10081165.
8 E. Ferraz, J. Coroado, J. Gamelas, J. Silva, F. Rocha and A. Velosa, Spent Brewery Grains for Improvement of Thermal Insulation of Ceramic Bricks, *J. Mater. Civ. Eng.*, 2013, **25**(11), 1638–1646, DOI: 10.1061/(asce)mt.1943-5533.0000729.
9 O. S. Stamenković, K. S. Siliveru, V. B. V. Veljkovic, I. B. B. Banković-Ilić, M. B. T. Tasić, I. A. C. Ciampitti, I. G. D. Đalović, P. M. M. Mitrović, V. S. S. Sikora and V. P. Prasad, Production of biofuels from sorghum, *Renewable Sustainable Energy Rev.*, 2020, **124**(5), 109769, DOI: 10.1016/j.rser.2020.109769.
10 Z. Zhu, L. Rosendahl, S. S. Toor, D. Yu and G. Chen, Hydrothermal liquefaction of barley straw to bio-crude oil: effects of reaction temperature and aqueous phase

recirculation, *Appl. Energy*, 2015, **137**, 183–192, DOI: 10.1016/j.apenergy.2014.10.005.

11 F. Gronwald and L. Wang, Advancing Renewable Energy: The Prospects of Hydrothermal Liquefaction (HTL) for Biomass into Bio-Oil Conversion, *Int. J. Environ. Eng. Educ.*, 2024, **6**(3), 132–144.

12 Y. Yue, J. R. Kastner and S. Mani, Two-Stage Hydrothermal Liquefaction of Sweet Sorghum Biomass – Part II: Production of Upgraded Biocrude Oil, *Energy Fuels*, 2018, **32**(7), 7620–7629, DOI: 10.1021/acs.energyfuels.8b00669.

13 S. S. Toor, L. Rosendahl and A. Rudolf, Hydrothermal liquefaction of biomass: a review of subcritical water technologies, *Energy*, 2011, **36**(5), 2328–2342, DOI: 10.1016/j.energy.2011.03.013.

14 S. Karagöz, T. Bhaskar, A. Muto, Y. Sakata and M. A. Uddin, Low-temperature hydrothermal treatment of biomass: effect of reaction parameters on products and boiling point distributions, *Energy Fuels*, 2004, **18**(1), 234–241, DOI: 10.1021/ef030133g.

15 F. A. Oghyanous and C. Eskicioglu, Hydrothermal liquefaction *vs.* fast/flash pyrolysis for biomass-to-biofuel conversion: new insights and comparative review of liquid biofuel yield, composition, and properties, *Green Chem.*, 2025, **27**, 7009–7041, DOI: 10.1039/d5gc01314c.

16 S. Karagöz, T. Bhaskar, A. Muto and Y. Sakata, Hydrothermal upgrading of biomass: effect of K_2CO_3 concentration and biomass/water ratio on products distribution, *Bioresour. Technol.*, 2006, **97**(1), 90–98, DOI: 10.1016/j.biortech.2005.02.051.

17 A. A. S. Shah, K. S. Sharma, M. S. H. Haider, S. S. T. Toor, L. A. R. Rosendahl, T. H. P. Pedersen and D. C. Castelleo, The Role of Catalysts in Biomass Hydrothermal Liquefaction and Biocrude Upgrading, *Processes*, 2022, **10**(2), 207, DOI: 10.3390/pr10020207.

18 D. Egesa, Process intensification of biofuel production from microalgae applying magnetic nanoparticles, PhD dissertation, University of Bath, 2019.

19 M. Scarsella, B. de Caprariis, M. Damizia and P. De Filippis, Heterogeneous catalysts for hydrothermal liquefaction of lignocellulosic biomass: a review, *Biomass Bioenergy*, 2020, **140**, 105662, DOI: 10.1016/j.biombioe.2020.105662.

20 B. Zhao, *et al.*, Synergistic effects of metallic Fe and other homogeneous/heterogeneous catalysts in hydrothermal liquefaction of woody biomass, *Renewable Energy*, 2021, **176**, 543–554, DOI: 10.1016/j.renene.2021.05.115.

21 H. Durak and S. Genel, Hydrothermal liquefaction of *Sinapis arvensis* biomass using TiO_2-supported metal catalysts: a study on bio-oil yield and composition, *J. Supercrit. Fluids*, 2025, **227**(8), 106745, DOI: 10.1016/j.supflu.2025.106745.

22 A. Rojas-Pérez, *et al.*, Catalytic effect of ultrananocrystalline Fe_3O_4 on algal bio-crude production *via* HTL process, *Nanoscale*, 2015, **7**(42), 17664–17671, DOI: 10.1039/c5nr04404a.

23 B. Hao, D. Xu, G. Jiang, T. A. Sabri, Z. Jing and Y. Guo, Chemical reactions in the hydrothermal liquefaction of biomass and in the catalytic hydrogenation upgrading of biocrude, *Green Chem.*, 2021, **23**(4), 1562–1583, DOI: 10.1039/d0gc02893b.

24 X. Zhao, *et al.*, Recent Progress in Pd-Based Nanocatalysts for Selective Hydrogenation, *ACS Omega*, 2022, **7**(1), 17–31, DOI: 10.1021/acsomega.1c06244.

25 F. Pattnaik, K. Dhalsamant, S. Nanda and A. K. Dalai, Biomass and Bioenergy Catalytic hydrothermal liquefaction of Wheat Straw and Chemical Profiling of Bio-Crude Oil, *Biomass Bioenergy*, 2025, **194**, 107643, DOI: 10.1016/j.biombioe.2025.107643.

26 I. Mazariegos, E. Abdelfath-Aldayyat, S. Gonzalez-Rojo and X. Gomez, Reducing fossil fuel demand by using biofuels as an alternative hydrothermal liquefaction is a promising process for transforming biomass into, *RSC Sustainable*, 2025, **3**(6), 3228–3265, DOI: 10.1039/d5su00148j.

27 A. S. Chauhan, A. Kumar, R. Bains, M. Kumar and P. Das, A comprehensive study of palladium-based catalysts on different supports for the hydrogenolysis of 5-hydroxymethylfurfural (HMF) to 2,5-dimethylfuran (DMF) biofuel, *Biomass Bioenergy*, 2024, **185**, 107209, DOI: 10.1016/j.biombioe.2024.107209.

28 S. Zonoubi, M. Barati, M. Ghanbari and M. Hamadanian, H_2-free hydrodeoxygenation of microalgae biomass using Pd-Ni/γ-Al_2O_3 bimetallic nanocatalyst in the supercritical environment, *Sci. Rep.*, 2025, **15**, 1–18.

29 F. P. Sejie, O. A. Oyetunji, B. C. E. Makhubela, J. Darkwa and N. H. De Leeuw, Evaluation of Cobalt, Nickel, and Palladium Complexes as Catalysts for the Hydrogenation and Improvement of Oxidative Stability of Biodiesel, *Catalysts*, 2024, **14**(9), 653.

30 J. Ahmed, M. Sajjad, H. Abdullah Shakir, M. Khan, M. Franco, and M. Irfan, Magnetic Nanocatalysts for Biofuel Production, in *Agricultural Biomass Nanocatalysts for Green Energy Applications*, Springer Singapore, 2024, DOI: 10.1007/978-981-97-1623-4_7.

31 K. A. Rogers and Y. Zheng, Selective Deoxygenation of Biomass-Derived Bio-oils within Hydrogen-Modest Environments: A Review and New Insights, *ChemSusChem*, 2016, **9**(14), 1750–1772, DOI: 10.1002/cssc.201600144.

32 J. L. Lyon, D. A. Fleming, M. B. Stone, P. Schiffer and M. E. Williams, Synthesis of Fe oxide core/Au shell nanoparticles by iterative hydroxylamine seeding, *Nano Lett.*, 2004, **4**(4), 719–723, DOI: 10.1021/nl035253f.

33 M. Kashimalla, S. Suraboyina, V. Dubbaka and A. Polumati, Optimisation of a catalytic hydrothermal liquefaction process using central composite design for yield improvement of bio-oil, *Biomass Convers. Biorefin.*, 2021, **13**(5), 3751–3763, DOI: 10.1007/s13399-021-01451-8.

34 J. Watson, J. Lu, R. de Souza, B. Si, Y. Zhang and Z. Liu, Effects of the extraction solvents in hydrothermal liquefaction processes: biocrude oil quality and energy conversion efficiency, *Energy*, 2019, **167**, 189–197, DOI: 10.1016/j.energy.2018.11.003.

35 J. Nallasivam, B. E. Eboibi, A. Isdepsky, M. Lavanya, S. Bhaskar and S. Chinnasamy, Hydrothermal liquefaction of water hyacinth (*Eichhornia crassipes*): influence of reaction temperature on product yield, carbon and energy

recovery, and hydrocarbon species distribution in biocrude, *Biomass Convers. Biorefin.*, 2022, **12**(9), 3827–3841, DOI: 10.1007/s13399-020-01032-1.

36 EN14104, *Determination of Acid Value for Fat and Oil Derivatives*European Committee for Standardization, 2003, vol. **1**, no. I.

37 ISO, International Standard ISO 3961. Animal and Vegetable Fats and Oils—Determination of Iodine Value, 2018, vol. **6**, pp. 1–9, Online, Available: https://www.iso.org/obp.

38 D. T. Adeyemi, A. Saleh, F. B. Akande, O. O. Oniya and F. A. Ola, Determination of Fuel Properties of Biodiesel from Sand Apple Seed Oil with Automotive Gas Oil Blend, *J. Appl. Sci. Environ. Manage.*, 2021, **25**(8), 1365–1369, DOI: 10.4314/jasem.v25i8.12.

39 K. Mishra, N. Basavegowda and Y. R. Lee, Biosynthesis of Fe, Pd, and Fe–Pd bimetallic nanoparticles and their application as recyclable catalysts for [3 + 2] cycloaddition reaction: a comparative approach, *Catal. Sci. Technol.*, 2015, **5**(5), 2612–2621, DOI: 10.1039/c5cy00099h.

40 F. Gulbagca, A. Aygün, M. Gülcan, S. Ozdemir, S. Gonca and F. Şen, Green synthesis of palladium nanoparticles: preparation, characterization, and investigation of antioxidant, antimicrobial, anticancer, and DNA cleavage activities, *Appl. Organomet. Chem.*, 2021, **35**(8), 1–9, DOI: 10.1002/aoc.6272.

41 B. de Caprariis, M. Scarsella, I. Bavasso, M. P. Bracciale, L. Tai and P. De Filippis, Effect of Ni, Zn and Fe on hydrothermal liquefaction of cellulose: Impact on bio-crude yield and composition, *J. Anal. Appl. Pyrolysis*, 2021, **157**, 105225, DOI: 10.1016/j.jaap.2021.105225.

42 R. Bao, *et al.*, A Review of Hydrothermal Biomass Liquefaction: Operating Parameters, Reaction Mechanism, and Bio-Oil Yields and Compositions, *Energy Fuels*, 2024, **38**(10), 8437–8459, DOI: 10.1021/acs.energyfuels.4c00240.

43 Y. Zhang, X. Zhu and B. Zhang, Biomass to Biocrude: A Brief Review of Catalytic, *Bioresources*, 2025, **20**(4), 11295–11318, DOI: 10.15376/biores.20.4.Zhang.

44 M. Kashimalla and A. Polumati, *Hydrothermal Liquefaction of Sorghum Bagasse for Maximization of Bio-Crude Using Homogeneous Catalyst (Na2CO3)*, 2022, DOI: 10.21203/rs.3.rs-1452608/v1.

45 G. Liu, *et al.*, Evaluation of Storage Stability for Biocrude Derived from Hydrothermal Liquefaction of Microalgae, *Energy Fuels*, 2021, **35**(13), 10623–10629, DOI: 10.1021/acs.energyfuels.1c01386.

46 T. H. Seehar, S. S. Toor, A. A. Shah, T. H. Pedersen and L. A. Rosendahl, Biocrude production from wheat straw at sub and supercritical hydrothermal liquefaction, *Energies*, 2020, **13**(12), 3114, DOI: 10.3390/en13123114.

47 ASTM D6751, ASTM D6751. Standard Specification for Biodiesel Fuel Blend Stock (B100) for Middle Distillate Fuels. – Date of Introduction 2023-03-01, 2023, pp. 1–7, DOI: 10.1520/D6751-20A.10.1520/D6751-23.

48 S. I. Umeh and P. A. Okonkwo, The Essential Properties of Oils for Biodiesel Production, in *Biodiesel Plants – Fueling the Sustainable Outlooks*. ed. E. Jacob-Lopes, L. Q. Zepka, and C. D. Mariany, IntechOpen, 2025, p. 116, DOI: 10.5772/intechopen.1008694.

49 X. Yang, *et al.*, Analysis of Physicochemical Properties of Bio-Oil from Hydrothermal Liquefaction of Blackcurrant Pomace, *Bioresour. Technol.*, 2020, **102**(7), 6765–6794, DOI: 10.1016/j.biortech.2011.06.041.

50 H. Wang, H. Tang, J. Wilson, S. O. Salley and K. Y. S. Ng, Total acid number determination of biodiesel and biodiesel blends, *J. Am. Oil Chem. Soc.*, 2008, **85**(11), 1083–1086, DOI: 10.1007/s11746-008-1289-8.

51 A. K. Sodhi, S. Tripathi and K. Kundu, Biodiesel production using waste cooking oil: a waste to energy conversion strategy, *Clean Technol. Environ. Policy*, 2017, **19**(6), 1799–1807, DOI: 10.1007/s10098-017-1357-6.